Journal of Nuclear Medicine, published on May 10, 2019 as doi:10.2967/jnumed.118.222844

Imaging metastatic castration-resistant prostate cancer patients with ^{89}Zr-DFO-MSTP2109A anti-STEAP1 antibody

Jorge A. Carrasquillo[1,2,3], Bernard M. Fine[4], Neeta Pandit-Taskar[1,2,3], Steven M. Larson[1,2,3], Stephen E. Fleming[1], Josef J. Fox[1], Sarah M. Cheal[1], Joseph A. O'Donoghue[5], Shutian Ruan[1], Govind Ragupathi[6], Serge K. Lyashchenko[7], John Humm[5], Howard I. Scher[6,8], Mithat Gönen[9] Simon P. Williams[4], Daniel C. Danila[6,8]*, Michael J. Morris[6,8]*

[1]Department of Radiology, Memorial Sloan Kettering Cancer Center, New York, New York; [2]Department of Radiology, Weill Cornell Medical Center, New York, New York; [3]Center for Targeted Radioimmunotherapy and Diagnosis, Ludwig Center for Cancer Immunotherapy, New York, New York; [4]Genentech, South San Francisco, California; [5]Department of Medical Physics, Memorial Sloan Kettering Cancer Center, New York, New York; [6]Department of Medicine, Memorial Sloan Kettering Cancer Center, New York, New York; [7]Radiochemistry and Molecular Imaging Probes Core, Memorial Sloan Kettering Cancer Center, New York, New York; [8]Joan and Sanford I. Weill Department of Medicine, Weill Cornell Medicine, New York, New York; and [9]Biostatistics Service, Department of Epidemiology and Biostatistics, Memorial Sloan Kettering Cancer Center, New York, New York.

*Contributed equally as co-senior authors.

Corresponding/First Author: Jorge A. Carrasquillo, MD
Memorial Sloan Kettering Cancer Center
1275 York Avenue, New York, NY 10065
Telephone: 212-639-2459; Fax: 212-717-3263
E-mail: carrasj1@mskcc.org

Running title: ^{89}Zr- anti-STEAP1 PET imaging

Research Support: This research was supported by The Ludwig Center for Cancer Immunotherapy, New York, NY; Genentech, Inc., and NCI grant P01 CA33049. The Clinical Grade Production (CGP) radiochemistry core facility at Memorial Sloan Kettering Cancer Center is funded in part through the NIH/NCI Cancer Center Support Grant P30 CA008748.

Disclosure of potential conflicts of interest: This study was supported by Genentech, Inc. (member of the Roche Group), which holds the right to the antibody; two co-authors are Genentech employees and hold stock in Roche (B. Fine and S. Williams). S.M. Larson has received commercial research grants from Genentech and J.A. Carrasquillo, M.J. Morris, N. Pandit-Taskar, and D.C. Danila have received research support from Genentech.

S.M. Larson also reports receiving commercial research grants from WILEX AG, Telix Pharmaceuticals Limited, and Regeneron Pharmaceuticals, Inc.; holding ownership interest/equity in Voreyda Theranostics Inc. and Elucida Oncology Inc., and holding stock in

ImaginAb, Inc. He is the inventor and owner of issued patents both currently unlicensed and licensed by MSK to Samus Therapeutics, Inc. and Elucida Oncology, Inc. S.M. Larson is or has served as a consultant to Cynvec LLC, Eli Lilly & Co., Prescient Therapeutics Limited, Advanced Innovative Partners, LLC, Gerson Lehrman Group, Progenics Pharmaceuticals, Inc., and Janssen Pharmaceuticals, Inc.

J.A. Carrasquillo has received funding support from Chugai Pharmaceuticals Co., Gilead, Regeneron Pharmaceuticals, and Algeta ASA, and has served as a consultant for Y-mAbs Therapeutics, Inc. and Bayer.

G. Ragupathi has served as a paid consultant and shareholder of MabVax Therapeutics Holdings, Inc. and Adjuvance Technologies.

J.A. O'Donoghue is or has served as a consultant to WILEX AG, Algeta ASA, and Janssen Pharmaceuticals, Inc.

M.J. Morris has served as an unpaid consultant to Astellas Pharma, Inc., Bayer AG, and Endocyte, Inc. and as a paid consultant to Advanced Accelerator Applications, Blue Earth Diagnostics, Tokai Pharmaceuticals, Inc., and Tolmar Pharmaceuticals, Inc., and has received institutional research funding for conducting clinical trials from Bayer AG, Sanofi, Endoycte, Inc., Progenics Pharmaceuticals, Inc., Corcept Therapeutics, Inc. He has also received funds for travel to academic meetings from Endocyte, Inc. and Bayer AG.

D. Danila has received research support from the US Department of Defense, American Society of Clinical Oncology, Prostate Cancer Foundation, Stand Up 2 Cancer, Janssen Research & Development, Astellas, Pfizer, Medivation, Agensys, and CreaTV. He has served as a consultant to Angle LLT, Janssen Research & Development, Astellas, Medivation, Agensys, and ScreenCell.

All other authors have no competing interests.

Word count: 5,924

ABSTRACT

Six-transmembrane epithelial antigen of prostate-1 (STEAP1) is a relatively new identified target in prostate cancer. We evaluated the ability of PET/CT with ^{89}Zr-DFO-MSTP2109A, an antibody that recognizes STEAP1, to detect lesions in patients with metastatic castration-resistant prostate cancer (mCRPC).

Methods: Nineteen mCRPC patients were prospectively imaged using ~185 MBq/10mg of ^{89}Zr-DFO-MSTP2109A. ^{89}Zr-DFO-MSTP2109 PET/CT images obtained 4-7 days post-injection were compared to bone and CT scans. Uptake in lesions was measured. Fifteen patients were treated with an antibody-drug conjugate (ADC) based on MSTP2109A; ADC treatment-related data was correlated with tumor uptake by PET imaging. Bone and/or soft tissue biopsies were evaluated.

Results: No significant toxicity occurred. Excellent uptake was observed in bone and soft tissue disease. Median SUVmax was 20.6 in bone and 16.8 in soft tissue. Sixteen of 17 lesions biopsied were positive on ^{89}Zr-DFO-MSTP2109A and all sites were histologically positive (one on repeat biopsy). Bayesian analysis resulted in a best estimate of 86% of histologically positive lesions being true positive on imaging (95% confidence interval of 75%-100%). There was no correlation between SUVmax tumor uptake and STEAP1 IHC, survival following ADC treatment, number of ADC treatment cycle, or change in PSA.

Conclusions: ^{89}Zr-DFO-MSTP2109A is well tolerated and shows localization in mCRPC sites in bone and soft tissue. Given the high SUV in tumor and localization of a large number of lesions, this reagent warrants further exploration as a companion diagnostic in patients undergoing STEAP1-directed therapy.

Key words: STEAP1, ^{89}Zr-, antibody, positron, prostate cancer

INTRODUCTION

Prostate cancer-selective antigens have been identified as targets for imaging and/or therapeutic intervention, including prostate-specific membrane antigen (PSMA) (*1-7*) and prostate stem cell antigen (PSCA) (*8*). Six-transmembrane epithelial antigen of prostate (STEAP) comprises a family of four novel cell surface markers that are highly expressed in prostate cancer but also present in other cancers and have little cross-reactivity to other normal tissues (*9-11*). STEAP1 is a novel 339 amino acid cell surface marker. Its exact function has yet to be determined, but it appears to be an ion channel or transporter protein with a role in cell adhesion and may be related to tumor proliferation and invasiveness (*9*). A role in intracellular communication and tumor growth inhibition *in vivo* has been shown, as well as a possible role in iron metabolism (*11*). Previous reports suggest STEAP1 expression may be a biomarker for worse prognosis of prostate cancer (*12*).

Because of high expression in prostate and other cancers, STEAP1 has been identified as a promising candidate for therapeutic intervention using antibody drug conjugates, monoclonal antibodies, DNA vaccines, and small non-coding RNAs (*13*). Preclinical studies with ^{111}In or ^{89}Zr-MSTP2109A anti-STEAP1, an internalizing antibody showed a correlation between the expression of STEAP1, radiolabeled antibody tumor uptake, and ADC efficacy; although in one cell line, high target expression identified by imaging and immunohistochemistry (IHC) showed weak efficacy (*14*). The latter report suggested that radioimmunoimaging may be used to inform efficacy of ADC in patients considered for treatment and led to a phase I trial with DSTP3086S, a monomethyl auristatin E (MMAE) conjugated to MSTP2109A anti-STEAP1 antibody

(ClinicalTrials.gov identifier NCT01283373) based on the same MSTP2109A antibody described in this report. In addition, ^{89}Zr-DFO-MSTP2109A has detected changes in STEAP1 induced by anti-androgen therapy (*15*).

In this report, we evaluated the ability of ^{89}Zr-DFO-MSTP2109A to image STEAP1 in patients with metastatic castration-resistant prostate cancer (mCRPC). A separate report will describe the pharmacokinetics, detailed biodistribution, and dosimetry of ^{89}Zr-DFO-MSTP2109A in the initial 6 patients enrolled.

MATERIALS and METHODS

Patient eligibility and protocol design

This was a prospective single-center phase I/II imaging study using ^{89}Zr-positron labeled DFO-MSTP2109A, an anti-STEAP1 antibody in 19 patients with mCRPC. Our institutional review board approved the study and all patients gave written informed consent (ClinicalTrials.gov identifier NCT01774071). All patients required histologically confirmed progressing mCRPC with documented metastatic disease on bone scan, computed tomography (CT), and/or magnetic resonance imaging (MRI) according to prostate cancer working group 2 (PCWG2) criteria. Patients had a Karnofsky score of >60%, platelet $\geq$75 K/microL, absolute neutrophil $\geq$1.0 K/microL, bilirubin <1.5 upper limit of normal (ULN), ALT/AST <2.5 ULN, and eGFR >30 ml/min/1.73 m^2. All patients had IHC determination of STEAP1 antigen presence of 1+ and above on tumor tissue (Ventana Medical Systems, Tucson, AZ); in addition, most patients had research biopsies just before ^{89}Zr-DFO-MSTP2109A imaging or shortly afterward as part of another research protocol or as clinically indicated.

A parallel therapeutic phase I trial with DSTP3086S ADC based on monomethyl auristatin conjugated to MSTP2109A (ClinicalTrials.gov identifier NCT01283373) was also accruing at our institution (*16*). Fifteen of our patients were subsequently enrolled onto the DSTP3086S trial with the other four no longer meeting entry criteria for the ADC trial. The ADC trial is not the subject of this report and will be reported elesewhere.

Antibody characteristics

MSTP2109A is a humanized IgG1 monoclonal antibody that binds to STEAP1. It was produced under good manufacturing practice (GMP) (Genentech, South San Francisco, CA) and conjugated with desferrioxamine (DFO) under GMP conditions by the Memorial Sloan Kettering (MSK) Clinical Grade Production (CGP) core facility (*17*). The antibody was radiolabeled with ^{89}Zr (a positron emitter with a 78.4-hour radioactive half-life) by MSK's Radiochemistry and Molecular Imaging Probe Core Facility using methods previously described (*18*), in compliance with the requirements specified in the Chemistry, Manufacturing, and Controls section of an FDA-approved IND (#116,724).

Imaging and whole-body analysis

All patients underwent delayed imaging at a median of 6 days post-injection (range 4 to 7 days). This imaging time was based on serial biodistribution and pharmacokinetic evaluation conducted on the first 6 patients (data not shown) who received the same antibody activity and mass as the subsequent patients. Imaging was performed on a General Electric DSTE positron emission

tomography (PET(/CT) scanner in 3D mode using iterative reconstruction with attenuation, scatter, and other standard corrections applied as for clinical FDG imaging. Images were obtained from the top of the skull to the proximal thigh using a median of 7 minutes per field of view (FOV).

^{89}Zr-DFO-MSTP2109A images were read independently by three experienced nuclear medicine physicians, two of whom were completely blinded to any data or imaging (NPT and SML) and a third (JAC) who had previously reviewed the patient history, because he was the principal investigator of the trial, but had not reviewed any images. A standardized form for bone and soft tissue lesion sites including organs and nodes was used for reading the three different scans (^{89}Zr-DFO-MSTP2109A). Liver and lung sites were assigned to right and left sides, and major lymph node regions were designated separately to neck, chest, abdomen, and pelvic regions. Images read as definitely positive or probably positive were considered positive; those read as unsure, probably negative, or definitely negative were considered negative. Sites deemed positive by at least two of the three readers were considered positive.

Localization in tumor was defined as focal accumulation greater than adjacent or contralateral background in areas where physiologic activity was not expected. All images and maximum intensity projection (MIP) images were reviewed on a dedicated PET analysis workstation (AWS GE Healthcare, Waukesha, WI or Hermes Medical Solutions, Stockholm, Sweden). Volumes of interest (VOIs) were placed visually over bone and/or soft tissue tumors and atrial blood pool. Maximum standardized uptake value (SUVmax) or mean standardized uptake value (SUVmean) normalized to body weight [(kBq/mL activity in region)/(kBq injected activity/body weight in g)] was obtained using HERMES software. For correlation to IHC, we also determined SUVpeak in

addition to SUVmax in the site of fresh lesion biopsies. Separate readers, blinded from all other studies, identified positive sites of tumor uptake using the above-described scale in bone scan (JJF) or CT scan (SEF).

Evaluation for toxicity

Patients' vital signs were monitored at baseline before injection and every 30 minutes for 2 hours post-injection and at the 4- to 7-day imaging time. Adverse events were documented using CTCAE V4 criteria. Safety assessment was performed from the period of informed consent to one week post-administration of ^{89}Zr-DFO-MSTP2109A.

STATISTICS

Descriptive statistics included median or mean, standard deviation, and correlation. Statistical comparison between groups was performed using paired t-test and Pearson or Spearman correlation coefficient using SigmaStat 3.5 (Systat Software Inc, San Jose, CA). Because no gold standard was available, a known site of disease was defined as any lesion identified by bone scan or CT (bone or soft tissue); furthermore, any bone lesion seen on CT or bone scan was considered positive for conventional imaging modalities (CIM).

The presence of many lesions, of which only a small number can be biopsied, presents a challenge for imaging studies of multi-focal metastatic cancer and precludes the use of traditional metrics of diagnostic accuracy such as sensitivity and specific and predictive value. To partially remedy this, we have used a Bayesian approach to apply information gleaned from biopsied lesions to project

the number of cancerous lesions among the unbiopsied ones as described in the appendix of Pandit Taskar et al (*19*).This approach uses the Bayes theorem to calculate the conditional expectation of the number of cancerous lesions among unbiopsied sites given the proportion of cancerous lesions among biopsied sites. To formalize this line of thinking, we denote by θ the probability that an imaged lesion is cancerous. Prior to observing the biopsy data, we have no information on θ other than the fact that it must be between 0 and 1. We represent this by a uniform distribution, also known as a beta distribution with shape and scale parameters equal to 1:

$P(\theta) \sim Beta(1,1)$

If there are n sites biopsies and x of them are histology and PET +, the likelihood function can be written as

$P(X) \sim Bin(n,X)$

And the posterior distribution of θ is now

$P(\theta|X) \sim Beta(X+1, n-X+1)$

This distribution is used to derive an estimate for θ (posterior mean) as well as a confidence interval (highest posterior density region). The marginal distribution of θ can then be used to make predictions about the expected number of positive lesions among unbiopsied lesions. This requires

the assumption that prevalence of positive lesions is similar among biopsied and unbiopsied lesions.

RESULTS

Radiolabeling

The mean radiosynthesis yield was 81% (n=19, range 64-92%). The product radiochemical purity was 99.8% (range: 98.7-100%), as measured by radio-TLC. The median specific activity of the radiolabeled product was 88 MBq/mg (range: 67-1283 MBq/mg). The median immunoreactivity fraction was 96% (range: 91-99%), as determined by a Lindmo type assay, using 293/STEAP1c.LB50 cells supplied by Genentech, Inc. Patients received a median injection of 185 MBq (range 170-199 MBq) containing a median mass of 2.39 mg (range: 1.87-2.92 mg) of the radiolabeled ^{89}Zr-DFO-MSTP2109A, which was supplemented with the non-radiolabeled carrier DFO-MSTP2109A for a total antibody administered mass of 10 mg. In accordance with the criteria in our protocol, we did not evaluate higher mass of antibody given that the median volume of distribution was close to plasma volume and the lowest beta T1/2 in plasma was long (105 h, suggesting there was not a large normal antigen “sink” and furthermore, high-contrast imaging was obtained with the 10 mg.

Patients

A total of 20 patients provided written informed consent, but 1 patient declined to participate. Thus, 19 consecutive patients were analyzed with a median age of 65 years old (range 47-79). Of

these patients, 6 underwent serial imaging and blood draws. Pharmacokinetics, time course of imaging, and dosimetry data will be reported separately. Nonetheless, a representative time course of uptake is shown in Supplementary Figure 1 that also describes the normal biodistribution. The blood pool in early images decreased considerably over time (Supplementary Fig. 1), particularly in patients with extensive bone involvement (Fig. 1).

IHC grading for STEAP1 on fresh and/or archival tissue showed 3+ (n=6), 2+ (n=9), and 1+ (n=4). All patients had a baseline prostate-specific antigen (PSA) determination within two weeks prior to antibody injection and a median PSA of 30.5 ng/mL (range 1.0-1806 ng/mL). All patients had a median of 4 (range 2-8) prior prostate-directed therapeutic regimens. Fifteen patients subsequently participated in a separate protocol using escalating doses of DSTP3086S ADC (MSTP2109 antibody-based drug conjugate) and received 1-21 cycles of treatment with the ADC (median 5). Six of these patients came off of the ADC due to adverse events (AE) from ADC, whereas 9 remained on the drug until progression, thus limiting assessment due to the small number of patients evaluable for response.

Patient-based analysis

The distribution of bone lesions per patient is shown in Table 1. All patients were considered positive for bone lesions on ^{89}Zr-DFO-MSTP2109A, although one (Patient 17) had a single bone lesion on ^{89}Zr-DFO-MSTP2109A. Eight patients were considered to have soft tissue disease on ^{89}Zr-DFO-MSTP2109A compared to 6 of 19 on CT (Table 1). Representative scans are shown in Figure 1, and distribution of soft tissue lesions is shown in Table 1.

Lesion-based analysis

Localization of ^{89}Zr-DFO-MSTP2109A in suspected bone metastases was observed in all patients (Table 1). A total of 515 sites were positive on ^{89}Zr-DFO-MSTP2109A.

Four patients underwent 5 biopsies of soft tissue sites positive on ^{89}Zr-DFO-MSTP2109A, each with confirmation of tumor involvement in biopsied sites. In 3 of these patients (Patients 13, 14, and 17), 3 biopsied tumors were only identified on ^{89}Zr-DFO-MSTP2109A (Supplementary Table 1). An example of soft tissue uptake is shown in Figure 2.

Quantitative analysis

Analysis of the bone lesions (n=18 patients) with the highest ^{89}Zr-DFO-MSTP2109A uptake showed a median SUVmax of 20.6 (range SUVmax 4.4-59.3; Supplementary Table 1). Patient 4 had a low SUVmax of 4.4 in the hottest bone lesion; this patient was atypical with poorly differentiated prostate cancer at 47 years of age. Analysis of the highest SUVmax in any soft tissue lesion per patient (n=9) showed a median SUVmax of 16.8 (range SUVmax 9.0-24.0; Supplementary Table 1).

The extent of bone involvement on ^{89}Zr-DFO-MSTP2109A varied and was easily identified visually. Patients with the most extensive bone disease had faster blood clearance of the antibody (Figs. 1, 3). A significant negative correlation between the number of bone lesions identified and the amount of activity in the blood (SUVmean) was evident on the last day of imaging, which ranged from 4 to 7 days (Pearson correlation coefficient: $p < 0.0001$, $r = -0.78$, $n = 19$). When only

patients whose last scan was at 6 days (n=16) were analyzed, the correlation was even more marked (Pearson correlation coefficient: $p<0.0001$, $r=-0.91$) (Fig. 3).

Various correlations were performed to determine if tumor uptake was related to IHC levels, PSA levels (possible index of tumor burden), or indices of tumor response in patients undergoing DSTP3086S ADC (Supplementary Table 2). SUVmax in tumor did not correlate with time from injection to time of death, time on study drug, number of DSTP3086S ADC treatment injections, baseline PSA levels, nadir PSA while on treatment with DSTP3086S ADC, or IHC level (Table 3). Because of potential differences between SUVmax and SUVpeak, we also correlated uptake in the six fresh biopsied lesions with their IHC status (Table 3).

Biopsy data

Because ethically or practically one cannot biopsy all suspicious ^{89}Zr-DFO-MSTP2109A sites, we relied on biopsies performed under other research protocols or for clinical indications either before (n=5) or after (n=12) ^{89}Zr-DFO-MSTP2109A imaging. Fifteen of 19 patients had 17 "contemporaneous" biopsies performed from 35 days prior to 71 days after injection of ^{89}Zr-DFO-MSTP2109A, showing ^{89}Zr-DFO-MSTP2109A uptake in 11 of 12 bone sites biopsied and all 5 soft tissue sites; all of these were performed prior to any ADC treatment (Supplementary Table 1). Pathology showed that all biopsied sites were positive for metastatic prostate cancer with the exception of one negative bone biopsy, which upon review of the CT-guided interventional biopsy images was attributed to the biopsy being performed on tissue immediately superior to the ^{89}Zr-DFO-MSTP2109A site. This site was strongly suspected to be metastatic as it was also positive on both FDG imaging and ^{89}Zr-anti-PSMA antibody scan (*19*) (data not shown), and a repeat

biopsy of this site 220 days after ^{89}Zr-DFO-MSTP2109A confirmed metastatic disease. The uptake of ^{89}Zr-DFO-MSTP2109A in the 12 contemporaneously biopsied sites in bone showed high uptake, with a median SUVmax of 10.7 (range 3.0-24.8; Supplementary Table 1), except for two biopsied tumor sites that had low SUV, including an expansive rib lesion in Patient 1 with SUVmax 3.2 and left iliac bone lesion (Patient 9, SUV 3.0). Four biopsied nodal sites in soft tissue had a median SUVmax of 11.9 (range 6.0-17.0). Other non-biopsied soft tissue sites that were also positive on antibody imaging and not identified on CT included nodes, usually small and/or in atypical location (supraclavicular and axillary), lung, liver, and prostatic bed.

Bayesian analysis

We applied Bayesian analysis to data obtained from bone biopsies to estimate the probability that a ^{89}Zr-DFO-MSTP2109A -positive bone lesion is biopsy-positive. There were 12 biopsies, 11 of which were positive for ^{89}Zr-DFO-MSTP2109A, which leads to a Bayesian estimate of 0.86 for the probability that a ^{89}Zr-DFO-MSTP2109A-positive bone lesion is biopsy-positive. The 90% Bayesian confidence interval for this estimate is 0.73 to 0.99. Supplementary Figure 2 demonstrates the probability density with our estimates marked.

Safety

A safety assessment was performed by serial measurement of blood pressure, heart rate, and temperature. No significant differences were observed for any of these parameters from baseline (one-way ANOVA: p=.067-0.98). Four patients had adverse events. Two patients had Grade 1 chills felt to be related to the antibody infusion on the day of injection, one of which was treated with diphenhydramine. One patient had nausea and vomiting and another had back pain, neither

of which were believed to be related to the study drug. Serious adverse events were noted in two patients: one occurred prior to antibody infusion and the other was sepsis due to urinary tract infection, which was considered unrelated to the study drug.

DISCUSSION

Overall, ^{89}Zr-DFO-MSTP2109A was well tolerated with very minor side effects attributable to the injected antibody and consistent with those observed with other antibodies such as low-grade fever and/or chills.

A prerequisite to using any antibody as an imaging agent is demonstrating its ability to localize in sites of disease. Preliminary preclinical studies showed good localization of ^{89}Zr-DFO-MSTP2109A in prostate xenografts (*14*). This study confirmed preclinical work and showed tumor localization of ^{89}Zr-DFO-MSTP2109A in tumor sites in all patients, extending the imaging findings from our preliminary report on 6 patients that focused on biodistribution, pharmacokinetics, and dosimetry. High-contrast localization was noted in both bone and soft tissue images in almost all patients when disease was present. This high uptake in bone (median SUVmax, 20.6; SUVmax: 59.3) compares favorably to that reported with ^{89}Zr-DFO-huJ591 anti-PSMA in prostate cancer (mean SUVmax: 8.9) or an ^{89}Zr-IAB2M anti-PSMA minibody (mean SUVmax: 13.8) (*19, 20*). The median SUVmax in soft tissue was 16.8 and maximum SUVmax was 24.0, which also compares favorably to the above-referenced antibodies that showed a mean SUVmax of 4.8 and 7 for ^{89}Zr-DFO-huJ591 and ^{89}Zr-IAB2M, respectively. An additional benefit compared to the latter anti-PSMA antibodies is that there is less normal liver accumulation, which facilitates seeing liver metastasis.

When CIM or bone scan only were used as a measure of bone involvement, the sensitivity of ^{89}Zr-DFO-MSTP2109A was 62% and 67%, respectively. The positive predictive value of ^{89}Zr-DFO-MSTP2109A in bone was 84% and 86% for CIM. In addition, 64% of bone sites identified only on ^{89}Zr-DFO-MSTP2109A probably corresponded to true sites identified on long-term follow-up CIM. These findings contrast with those we reported previously with ^{89}Zr-DFO-huJ591, which exhibited a higher sensitivity for tumor detection in bone than that we observed here. The reason for the discrepancy in these findings is not clear and may in part be related to differences in study population or possibly may indicate a difference in biological expression of STEAP1 vs. PSMA in mCRPC. Furthermore, the limitations of bone scans in identifying sites of viable bone disease versus treated non-viable disease are well recognized, as are the identification of false-positive sites. Additional limitations of this study are the small number of patients and that confirmation of all image-positive sites was not feasible for ethical reasons; thus, a gold standard for disease was not optimal. Despite these caveats, a large number of metastatic sites are identified as suggested not only by imaging but by biopsy correlation in numerous biopsied sites and by Bayesian analysis, which suggests the probability of 0.86 that a ^{89}Zr-DFO-MSTP2109A-positive site is biopsy-positive.

The sensitivity for detection of soft tissue lesions was 82% (Table 2). ^{89}Zr-DFO-MSTP2109A identified an additional 29 soft tissue lesions not detected on CT, whereas CT identified only 2 additional soft tissue lesions not detected on ^{89}Zr-DFO-MSTP2109A. With long-term follow-up, 41% of the 29 soft tissue sites identified on ^{89}Zr-DFO-MSTP2109A only were identified as abnormal, including 3 sites that were confirmed by biopsy. Compared to prior studies in prostate

cancer with ^{89}Zr-DFO-huJ591, our study showed a much higher sensitivity for detecting soft tissue tumor sites; furthermore, in contrast with ^{89}Zr-DFO-huJ591, more soft tissue sites were identified than with CT, some of which were confirmed on long-term follow-up (*19*).

While we have previously demonstrated with other antibodies that the degree of tumor uptake is related to tumor antigen concentration, in this study we did not establish a correlation of uptake with antigen based on IHC; this may be related to limitations in IHC and/or limitations of tumor sampling. Some variability in SUV in normal organs as well as tumor is expected, depending on the length of time from injection to imaging, and could affect correlations of uptake with various parameters. Furthermore, the more rapid removal of antibody from the circulation due to tumor accumulation could also interfere with the correlation of SUVmax with IHC. Nonetheless, we did observe that the presence of more ^{89}Zr-DFO-MSTP2109A-positive bone lesions was related to more rapid clearance of ^{89}Zr-DFO-MSTP2109A; although 10 mg of antibody was sufficient to result in high-contrast imaging in patients with mCRPC.

The quantitative analysis of SUV uptake did not correlate with treatment outcomes in patients receiving DSTP3086S ADC, including length of survival from treatment, number of treatments, or time on study. Although not statistically significant, there was a trend toward inverse correlation of SUVmax in any tissue and maximal % change in PSA with ADC treatment. This lack of correlation may have been related to the small number of patients examined, particularly because a significant number of patients (6 out of 15) discontinued ADC treatment due to side effects and overall there were only minor responses to ADC treatment (data not shown). However, these SUVs were used with a mechanistic pharmacokinetic model of DSTP3086A and preclinical studies of

MMAE to confirm that efficacious doses of the ADC toxin MMAE were potentially being delivered to many of the high-uptake lesions imaged. A typical tumor SUV of 20 was equivalent to several hundred nanomolars of antibody delivered to the tumor at the maximum therapeutic dose of 2.4 mg/kg. Even when allowing for significant deconjugation of MMAE from the ADC in circulation and a relatively rapid washout of free MMAE from the tumor, the tumor-free toxin concentration is likely to have been in the high tens of nanomolar, considerably above the IC50 concentration of around 1 nM in tumor cell lines. This finding suggests that disappointment in the patient's response rate was more likely caused by insufficient potency of MMAE in these patients' tumors (either innate or through resistance) than by limitations of tumor penetration and drug delivery.

This is the first study to report in detail on the imaging findings of targeting STEAP1, an antigen newly recognized to be overexpressed in prostate cancer. The difference we observed between targeting PSMA with ^{89}Zr-DFO-huJ591 and ^{89}Zr-DFO-MSTP2109A in patients with prostate cancer may possibly reflect differences related to the biology of STEAP1- vs. PSMA-positive prostate cancer. STEAP1 has not been as extensively studied as the PSMA antigen, and warrants further investigation. As stated above, lack of response to DSTP3086S ADC probably reflects an issue related to the potency of the ADC rather than delivery or presence of the STEAP1 antigen. Nonetheless, because of the excellent targeting of lesions and the novelty of STEAP1 in prostate cancer, we believe that this reagent warrants further evaluation in patients as a potential predictive biomarker for patients undergoing new STEAP1-directed therapy or as a means to identify patients who may be more amenable to STEAP1-directed treatment. While in this study we used 185 MBq, which results in relatively high radiation dose to normal organs, we feel that lower activities such

as 37 to 74 MBq used in other studies would be adequate for imaging while decreasing radiation dose.

ACKNOWLEDGMENTS

The authors wish to thank Jason Lewis, PhD, Chief of Radiochemistry and Imaging Sciences Service; Sonia Sequeira, PhD, Head of Product Development; Lee McDonald, PhD, Head of Investigational Products Core Facility; and Elisa de Stanchina, PhD, Head of Antitumor Assessment Core Facility for their support in drug development, as well as Amabelle Lindo, RN and Louise Harris, RN for nursing support; Bolorsukh Gansukh and Abigail Boswell for research support; Rashid Ghani, PharmD and the radiopharmacy group for radiopharmacy support; and Leah Bassity, MA and Garon Scott for their editorial expertise.

REFERENCES

1. Bander NH, Milowsky MI, Nanus DM, Kostakoglu L, Vallabhajosula S, Goldsmith SJ. Phase I trial of (177)lutetium-labeled J591, a monoclonal antibody to prostate-specific membrane antigen, in patients with androgen-independent prostate cancer. *J Clin Oncol.* 2005;23:4591-601.
2. Milowsky MI, Nanus DM, Kostakoglu L, Vallabhajosula S, Goldsmith SJ, Bander NH. Phase I trial of yttrium-90-labeled anti-prostate-specific membrane antigen monoclonal antibody J591 for androgen-independent prostate cancer. *J Clin Oncol.* 2004;22:2522-31.
3. Tagawa ST, Milowsky MI, Morris M, et al. Phase II study of lutetium-177-labeled anti-prostate-specific membrane antigen monoclonal antibody J591 for metastatic castration-resistant prostate cancer. *Clin Cancer Res.* 2013;19:5182-91.
4. Pandit-Taskar N, O'Donoghue JA, Beylergil V, et al. Zr-89-huJ591 immuno-PET imaging in patients with advanced metastatic prostate cancer. *Eur J Nucl Med Mol Imaging.* 2014;41:2093-105.
5. Kratochwil C, Bruchertseifer F, Rathke H, et al. Targeted alpha-therapy of metastatic castration-resistant prostate cancer with Ac-225-PSMA-617: dosimetry estimate and empiric dose finding. *J Nucl Med.* 2017;58:1624-31.
6. Kratochwil C, Giesel FL, Stefanova M, et al. PSMA-targeted radionuclide therapy of metastatic castration-resistant prostate cancer with Lu-177-labeled PSMA-617. *J Nucl Med.* 2016;57:1170-1176.
7. Afshar-Oromieh A, Holland-Letz T, Giesel FL, et al. Diagnostic performance of Ga-68-PSMA-11 (HBED-CC) PET/CT in patients with recurrent prostate cancer: evaluation in 1007 patients. *Eur J Nucl Med Mol Imaging.* 2017;44:1258-68.

8. Morris MJ, Eisenberger MA, Pili R, et al. A phase I/IIA study of AGS-PSCA for castration-resistant prostate cancer. *Ann Oncol.* 2012;23:2714-9.

9. Hubert RS, Vivanco I, Chen E, et al. STEAP: A prostate-specific cell-surface antigen highly expressed in human prostate tumors. *Proc Natl Acad Sci USA.* 1999;96:14523-8.

10. Moreaux J, Kassambara A, Hose D, Klein B. STEAP1 is overexpressed in cancers: A promising therapeutic target. *Biochem Biophys Res Commun.* 2012;429:148-55.

11. Gomes IM, Maia CJ, Santos CR. STEAP proteins: from structure to applications in cancer therapy. *Mol Cancer Res.* 2012;10:573-87.

12. Ihlaseh-Catalano SM, Drigo SA, de Jesus CMN, et al. STEAP1 protein overexpression is an independent marker for biochemical recurrence in prostate carcinoma. *Histopathology.* 2013;63:678-85.

13. Barroca-Ferreira J, Pais JP, Santos MM, et al. Targeting STEAP1 protein in human cancer: current trends and future challenges. *Curr Cancer Drug Targets.* 2018;18:222-30.

14. Williams SP, Ogasawara A, Tinianow JN, et al. ImmunoPET helps predicting the efficacy of antibody-drug conjugates targeting TENB2 and STEAP1. *Oncotarget.* 2016;7:25103-12.

15. Doran MG, Watson PA, Cheal SM, et al. Annotating STEAP1 regulation in prostate cancer with ^{89}Zr immuno-PET. *J Nucl Med.* 2014;55:2045-9.

16. Danila DC, Szmulewitz RZ, Baron AD, et al. A phase I study of DSTP3086S, an antibody-drug conjugate (ADC) targeting STEAP-1, in patients with metastatic castration-resistant prostate cancer (CRPC). *J Clin Oncol.* 2014;32.

17. Vosjan M, Perk LR, Visser GWM, et al. Conjugation and radiolabeling of monoclonal antibodies with zirconium-89 for PET imaging using the bifunctional chelate p-isothiocyanatobenzyl-desferrioxamine. *Nat Protoc.* 2010;5:739-43.

18. Holland JP, Sheh YC, Lewis JS. Standardized methods for the production of high specific-activity zirconium-89. *Nucl Med Biol.* 2009;36:729-39.

19. Pandit-Taskar N, O'Donoghue JA, Durack JC, et al. A phase I/II study for analytic validation of Zr-89-J591 immunoPET as a molecular imaging agent for metastatic prostate cancer. *Clin Cancer Res.* 2015;21:5277-85.

20. Pandit-Taskar N, O'Donoghue JA, Ruan ST, et al. First-in-human imaging with Zr-89-Df-IAB2M anti-PSMA minibody in patients with metastatic prostate cancer: pharmacokinetics, biodistribution, dosimetry, and lesion uptake. *J Nucl Med.* 2016;57:1858-64.

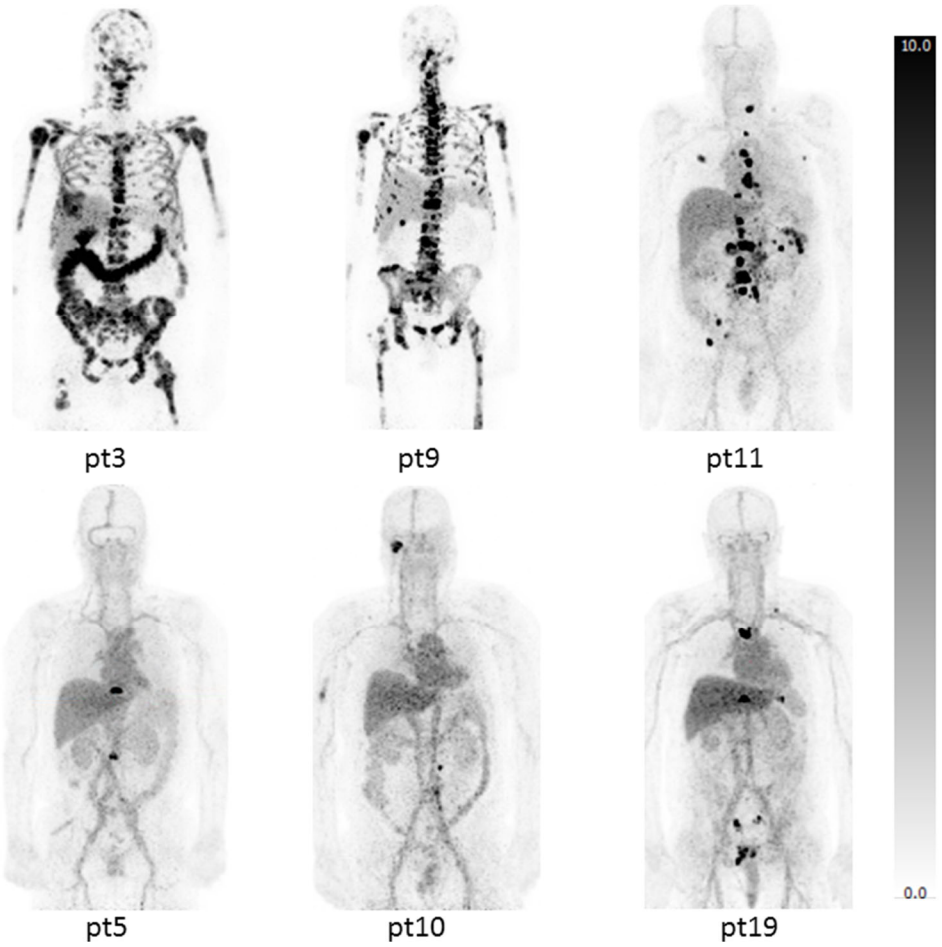

Figure 1. ^{89}Zr-DFO-MSTP2109A maximum-intensity projection images of selected patients with bone metastasis of various extent. Images were acquired at 6 days post-injection and are displayed at the same grayscale with an SUVmax of 10. Patients in the upper panel (particularly Patients 3 and 9) have extensive metastatic bone disease. Uptake in non-involved bone is low and not definitely seen in the projection images. Physiologic blood pool activity was prominent soon after injection and much less blood pool is seen in late images in those with more extensive bony disease. Uptake in liver is partially reflective of blood pool activity and parenchymal accumulation. Low-level uptake is also noted in the kidneys and variable uptake is noted in the bowel (intraluminal), which probably represents a route of excretion.

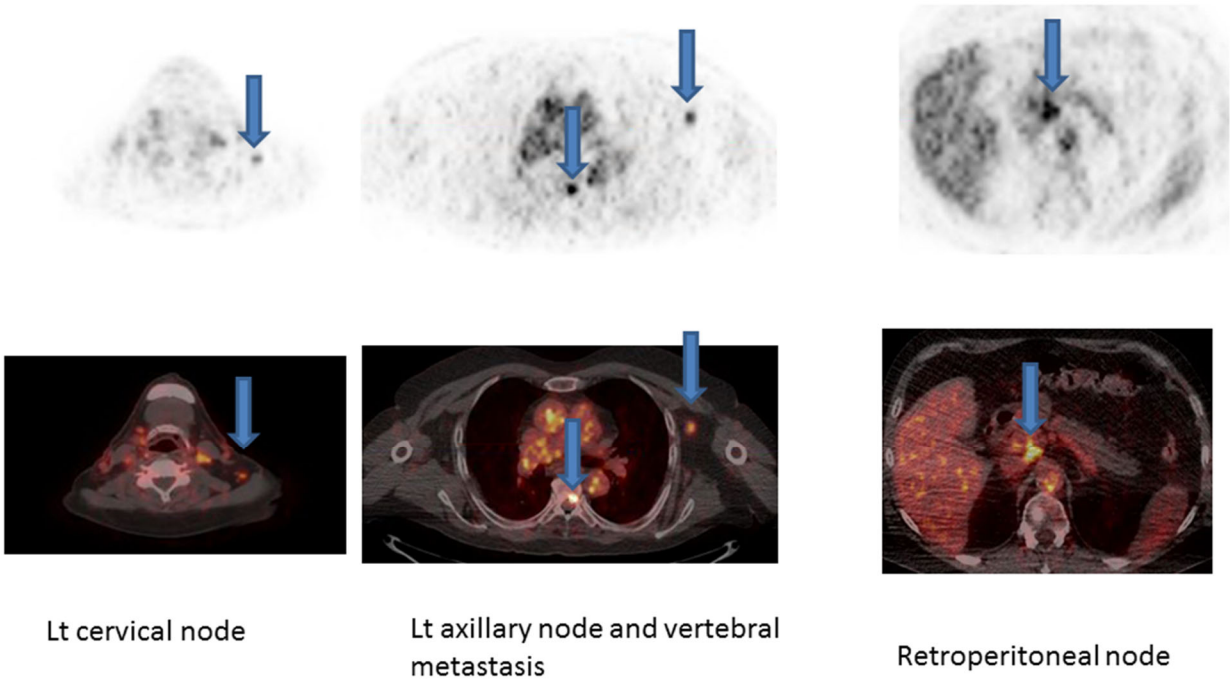

Figure 2. ^{89}Zr-DFO-MSTP2109A images of Patient 13 obtained 6 days post-injection. Images showed bone uptake in a vertebral lesion (middle panel, midline arrow), in addition to uptake in a left axillary node (middle panel arrow in left axilla) that was biopsy-proven metastatic disease. Left cervical nodal uptake (left panel, arrow) and retroperitoneal node (right panel, arrow) showed abnormal uptake; while these were negative on concurrent CT, follow-up FDG scan showed mild uptake at these sites.

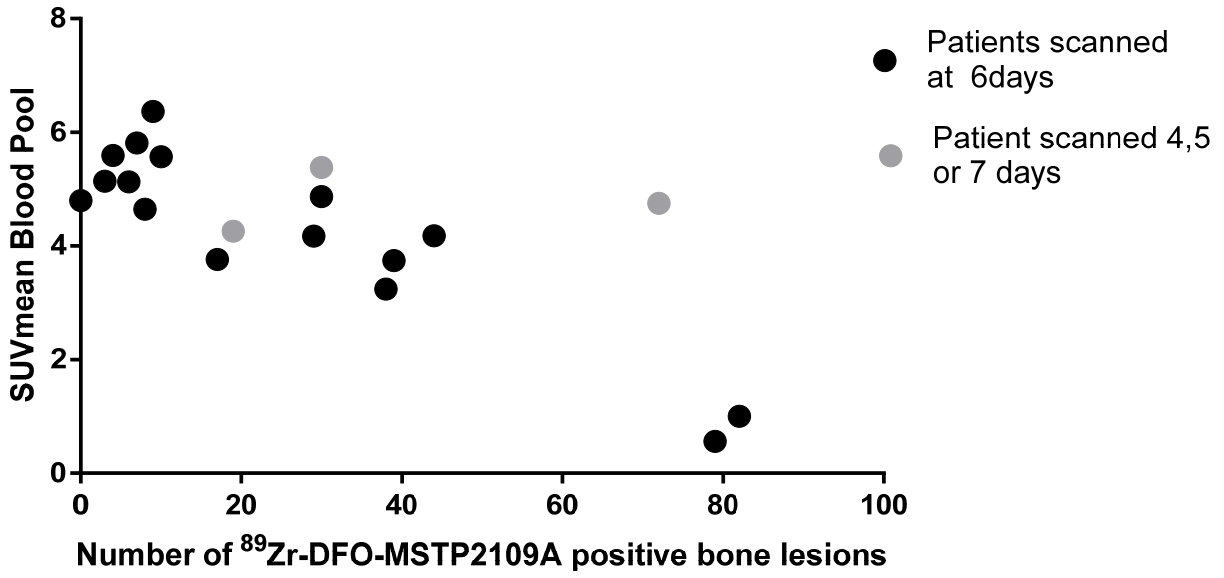

Figure 3. There was a negative correlation between number of lesions identified on ^{89}Zr-DFO-MSTP2109A and clearance of radioactivity from the blood pool. SUVmean in blood was lower in patients with a higher number of lesions when all patients (n=19) were considered (last scan 4-8 days) (Pearson correlation coefficient: r=-0.78, p=0.0001) or when patients were scanned on the most common day, which was 6 days (n=16 black dots) (Pearson correlation coefficient: r=-0.91, p<0.0001).

Table 1. Positive findings by imaging modality

	Bone lesions				Soft tissue*	
Patient #	^{89}Zr-DFO-MSTP2109A+	Bone scan+	CT+	CIM+	^{89}Zr-DFO-MSTP2109A+	CT+
1	34	31	16	32	1	1
2	71	73	7	73	0	0
3	80	88	74	88	6	2
4	8	54	50	66	0	0
5	3	4	5	8	0	0
6	32	41	17	45	0	0
7	27	30	22	31	0	0
8	40	84	71	85	0	0
9	83	80	31	80	5	1
10	4	2	0	2	2	2
11	17	14	7	14	8	3
12	8	30	10	33	0	0
13	9	22	17	25	4	0
14	5	6	13	14	6	0
15	30	38	37	51	0	0
16	20	11	4	11	0	0
17	1	0	0	0	6	2
18	32	27	14	31	0	0
19	11	15	18	19	0	0
Total	**515**	**650**	**413**	**708**	**38**	**11**

*Soft tissue lesions included nodes, liver, lung, and prostatic bed.

Table 2. Imaging findings by modality in bone or soft tissue lesions (n=19 patients)

Agent	Bone lesions						Soft tissue lesions		
	Bone scan +	Bone scan -	CT +	CT-	CIM +	CIM-	CT+	CT-	Total
^{89}Zr-DFO-MSTP2109A +	433	82	253	262 *	443	72	9	29	38
^{89}Zr-DFO-MSTP2109A -	217	48	160	105	265	NA	2	NA	
Total	650	130	413	367	708	72	11	29	

*24 sites identified on ^{89}Zr-DFO-MSTP2109A were not in CT field of view; 18 bone scan sites were not in CT field of view.

Table 3. Correlation between SUVmax in tumor vs. patient outcome, PSA, and IHC

Parameter compared to SUVmax	Correlation coefficient (n=number of patients)
Time from imaging injection to death	Pearson (n=19) r=-0.12, p=0.62
Time on DSTP3086S ADC treatment	Pearson (n=16) r=-0.59, p=0.054
Baseline PSA levels	Pearson (n=19) r=0.1, p= 0.67
Maximal PSA change post DSTP3086S ADC treatment compared to baseline	Pearson (n=16) r=-0.496, p=0.576
Highest IHC value (archival or fresh) vs. SUVmax	Spearman (n=19) r=0.37, p=0.12
IHC value fresh tissue vs. SUVmax	Spearman (n=6) r=0.0976, p=0.803
IHC value fresh tissue vs. SUVpeak	Spearman (n=6) r=-0.0976, p=0.803